Synthesis and Characterization of Anionic Amphiphilic Model Conetworks Based on Methacrylic Acid and Methyl Methacrylate: Effects of Composition and Architecture

Gergely Kali,[†,‡] Theoni K. Georgiou,[†] Béla Iván,[‡] Costas S. Patrickios,*[,†] Elena Loizou[⊥,§] Yi Thomann,[#] and Joerg C. Tiller[#]

Department of Chemistry, University of Cyprus, P.O. Box 20537, 1678 Nicosia, Cyprus; Department of Polymer Chemistry and Material Science, Institute of Materials and Environmental Chemistry, Chemical Research Center, Hungarian Academy of Sciences, P. O. Box 17, H-1525 Budapest, Pusztaszeri út 59-67, Hungary; Department of Chemistry, Louisiana State University, Baton Rouge, Louisiana 70803; Center for Neutron Research, National Institute of Standards and Technology, Gaithersburg, Maryland 20899; and Freiburg Materials Research Center and Institute for Macromolecular Chemistry, Department of Chemistry, University of Freiburg, Stefan-Meier-Str. 21, D-79104 Freiburg, Germany

Received October 18, 2006; Revised Manuscript Received January 4, 2007

ABSTRACT: A series of amphiphilic conetworks of methacrylic acid (MAA) and methyl methacrylate (MMA) were synthesized using group transfer polymerization (GTP). The MAA units were introduced via the polymerization of tetrahydropyranyl methacrylate (THPMA), followed by the removal of the protecting tetrahydropyranyl group by acid hydrolysis after network formation. 1,4-Bis(methoxytrimethylsiloxymethylene)-cyclohexane (MTSCH) was used as a bifunctional GTP initiator, while ethylene glycol dimethacrylate (EGDMA) served as the cross-linker. Nine of the conetworks were model conetworks, comprising copolymer chains between the cross-links of precise molecular weight and composition. Eight of the model conetworks were based on ABA triblock copolymers, while the ninth was based on a statistical copolymer. The tenth conetwork was not model but randomly cross-linked. The molecular weight and the composition of the linear conetwork precursors were analyzed by gel permeation chromatography and ^{1}H NMR, respectively, and were found to bear values close to the theoretically expected. FTIR spectroscopic analyses indicated complete polymerization of the EGDMA cross-linker vinyl units and complete hydrolysis of the THPMA units. The degrees of swelling (DS) of all the conetworks were measured in water and in THF as a function of the degree of ionization (DI) of the MAA units. The DSs in water increased with the DI of the MAA units (and the pH), while the DSs in THF presented the opposite trend. Finally, small-angle neutron scattering and atomic force microscopy confirmed nanophase separation in a triblock copolymer-based model conetwork and lack of it in its statistical copolymer counterpart.

Introduction

Amphiphilic polymer conetworks (APCN)[1−28] have attracted significant attention in recent years due to their unique structure, properties, and wide range of potential applications (see refs 1 and 2 for recent reviews). These include supports for enzymes with significantly improved catalytic activity,[3] templates for the preparation of inorganic nanoparticles,[4] matrices for controlled drug delivery,[5−8] scaffolds for tissue engineering[9−11] and implants,[12] materials for soft contact lenses,[13] where softness, mechanical strength,[14] and oxygen permeability[14,15] need to be combined, antifouling surfaces[16] and promoted release hosts,[17] and pervaporation membranes.[18] Because of their constitution of hydrophilic and hydrophobic polymer chains, APCNs are able to swell in and interact with both aqueous and organic media and can adsorb both polar and nonpolar solutes. Moreover, the immiscibility of their hydrophilic and hydrophobic components leads to phase separation at the nanoscale in APCNs.[3,4,19−22]

Another type of conetworks is that of model conetworks,[29] containing polymer chains of well-defined molecular weight and composition. Most of the APCNs reported in the literature so far cannot be considered as model conetworks because they comprise chains, between cross-linking points, with broad length distributions.[1] The synthesis of model APCNs can be accomplished by the use of "living" polymerization techniques,[30] such as "living" anionic, cationic, radical, and group transfer polymerizations (GTP). One of our research teams has developed a strategy for the synthesis of quasi-model (almost perfect; some defects are present) APCNs,[23−28] involving sequential addition of monomers and cross-linker under "living" polymerization conditions. In particular, we used GTP,[31−35] a rapid and facile "living" polymerization technique, to prepare quasi-model conetworks based on end-linked ABA triblock copolymers at room temperature.[24−27] This procedure was completed within only three polymerization/addition steps in a one-pot preparation. Most of our syntheses involved the use of a bifunctional GTP initiator and the sequential polymerization of two monomers: one hydrophilic and one hydrophobic.[24,25] These two monomers were commercially available and were the hydrophobic methyl methacrylate (MMA) and the hydrophilic positively ionizable 2-(*N*,*N*-dimethylamino)ethyl methacrylate (DMAEMA).[24,25] The swelling characterization of these APCNs led to the derivation of accurate structure−property relationships since all the conetworks possessed chains of well-defined structures.

* To whom correspondence should be addressed. E-mail: costasp@ucy.ac.cy.
[†] University of Cyprus.
[‡] Hungarian Academy of Sciences
[§] Louisiana State University.
[⊥] National Institute of Standards and Technology.
[#] University of Freiburg.

10.1021/ma062400y CCC: $37.00
Published on Web 02/21/2007

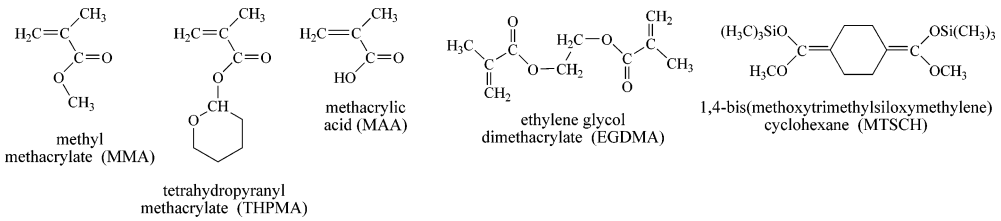

Figure 1. Chemical structures and names of monomers, cross-linker, and initiator used for the conetwork syntheses in this study.

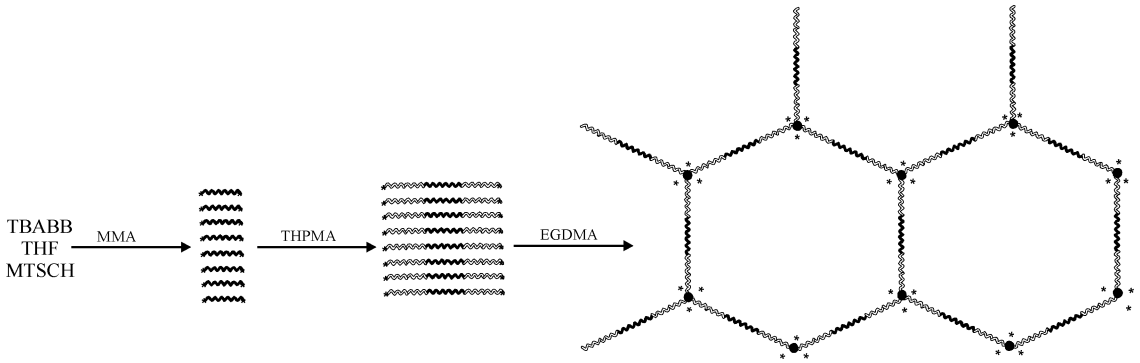

Figure 2. Schematic representation of the synthetic procedure for the preparation of the conetwork based on the MAA_{10}-*b*-MMA_{20}-*b*-MAA_{10} triblock copolymer (network 9, Table 1). The white color represents the MAA units, while the black color the MMA units. The stars indicate the "living" sites of the polymerization. The number of arms at the cross-links is not 3 (as the figure indicates) but around 30.[28]

The objective of the present work is to expand our previous investigations on model APCNs both on the synthetic and on the characterization sides. On the synthetic side, we explored the introduction of a negatively, rather than a positively, ionizable hydrophilic monomer, namely methacrylic acid (MAA). In contrast to DMAEMA, MAA cannot be polymerized directly by GTP and some other polymerization methods and requires chemical protection. This is one of the reasons why there are only a few reported examples of APCNs containing anionic, such as (meth)acrylic acid, units.[15] On the characterization side, in addition to the degrees of swelling (DS) in water, we also measured the DSs in THF over the whole range of degrees of ionization (DI) of MAA. Importantly, we introduced structural characterization of the nanophase behavior of uncharged conetworks by small-angle neutron scattering (SANS) and atomic force microscopy (AFM).

Experimental Section

Materials and Methods. The monomers, methyl methacrylate (MMA, hydrophobic, 96%) and methacrylic acid (MAA, hydrophilic and negatively ionizable, 98%), the cross-linker, ethylene glycol dimethacrylate (EGDMA, 98%), 3,4-dihydro-2*H*-pyran (DHP, 97%), tetrabutylammonium hydroxide (40% in water), benzoic acid (99.5%), calcium hydride (CaH_2, 90−95%), 2,2-diphenyl-1-picrylhydrazyl hydrate (DPPH, free radical inhibitor, 95%), basic alumina, and potassium metal (98%) were all purchased from Aldrich. The THPMA monomer was synthesized via catalytic esterification of MAA with 100% excess of DHP at 55 °C,[36] using a modification of the procedure reported by Hertler.[37] Thus, sulfuric acid rather than cross-linked poly(4-vinylpyridine hydrochloride) was used as the acid catalyst. Figure 1 shows the chemical structures and names of the monomers, the cross-linker, and the initiator used for the conetwork syntheses. Sodium metal was obtained from Fluka. Tetrahydrofuran (THF, 99.8%) was purchased from Labscan and was used both as the polymerization solvent (reagent grade) and as the mobile phase in chromatography (HPLC grade).

The solvent, THF, was dried by refluxing it over a potassium/sodium alloy for 3 days and was freshly distilled prior to polymerization. The monomers and the cross-linker were passed through basic alumina columns and were then stirred over CaH_2 in the presence of DPPH free-radical inhibitor to remove moisture and protic impurities. Then, these monomers were stored at 5 °C in the presence of DPPH to avoid undesired thermal polymerization. The monomers and the cross-linker were freshly distilled under vacuum and kept under a dry nitrogen atmosphere until use. The initiator, 1,4-bis(methoxytrimethylsiloxymethylene)cyclohexane (MTSCH), was synthesized according to the literature[38] and was distilled twice before use. The tetrabutylammonium bibenzoate (TBABB) catalyst was prepared by the method of Dicker et al.[33] and was stored under vacuum until use.

Polymerizations. All the conetworks in this study were synthesized by GTP. The reactions were carried out in 250 mL round-bottom flasks at room temperature. The polymerization exotherm was monitored using a digital thermometer to follow the progress of the reaction.

The polymerization procedure for the synthesis of one of the amphiphilic model conetworks (conetwork 9) is described in detail below, and it is depicted schematically in Figure 2. Freshly distilled THF (24 mL), MTSCH initiator (0.33 mL, 0.40 g, 1.15 mmol), and MMA (2.50 mL, 2.34 g, 23.4 mmol) were syringed in this order to a 250 mL round-bottom flask fitted with a rubber septum, kept under a dry nitrogen inert atmosphere. The polymerization was initiated by adding a small amount (∼10 mg, 20 μmol) of TBABB catalyst. The polymerization exotherm (22−31 °C) abated within 5 min, samples were withdrawn, and, subsequently, the second monomer, THPMA (3.9 mL, 3.9 g, 23.0 mmol), was charged slowly, giving an exotherm (23−35 °C). After sampling, EGDMA (1.75 mL, 1.84 g, 9.3 mmol) was added, resulting in gel formation within seconds and a temperature increase from 23 to 33 °C.

Characterization of the Conetwork Precursors. *Gel Permeation Chromatography.* The molecular weight distributions (MWD) and molecular weights (MW) of the linear homopolymer and copolymer precursors to the conetworks were determined by gel permeation chromatography (GPC). GPC was performed on a Polymer Laboratories chromatograph equipped with an ERC-7515A refractive index detector and a PL Mixed "D" column. The mobile phase was THF, delivered at a flow rate of 1 mL min^{-1} using a Waters 515 isocratic pump. The MW calibration curve was based on eight narrow MW (630, 2600, 4250, 13 000, 28 900, 50 000, 128 000, and 260 000 g mol^{-1}) linear PMMA standards (Polymer Laboratories).

^{1}H NMR Spectroscopy. The compositions of the conetwork precursors and the extractables from the conetworks were determined by ^{1}H NMR spectroscopy using a 300 MHz Avance Bruker

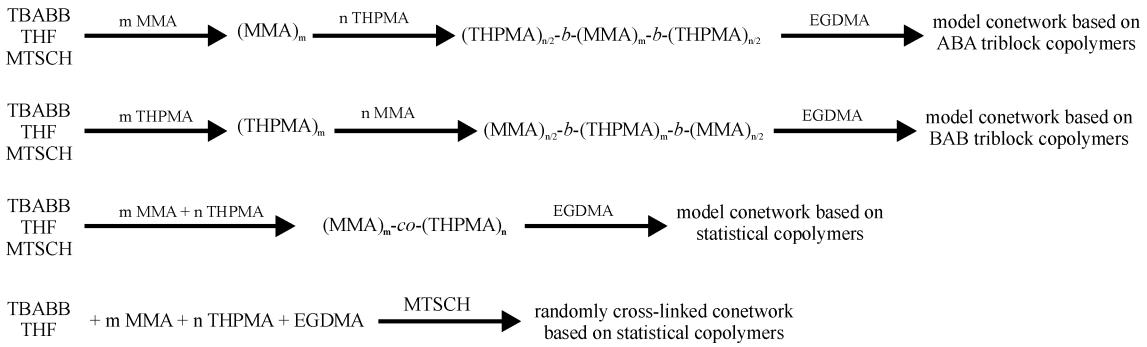

Figure 3. Synthetic routes for the preparation of four different conetwork architectures.

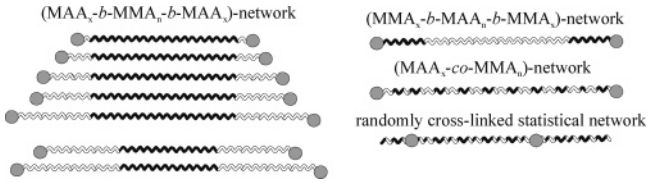

Figure 4. Schematic representation of the structure of the segments between the cross-links of the conetworks in this study. The white and black colors represent MAA and MMA chains, respectively. The EGDMA cross-linkers are shown as gray circles. Conetworks of the same architecture but different composition are shown in the left-hand-side column, while conetworks of different architectures with the same composition are exhibited on the right.

NMR spectrometer equipped with an Ultrashield magnet. The solvent was $CDCl_3$ containing traces of tetramethylsilane (TMS), which was used as an internal reference. ^{1}H NMR was also used to confirm the structure and the purity of the THPMA monomer and the MTSCH bifunctional initiator.

Determination of the Sol Fraction in the Conetworks. The resulting conetworks were removed from the polymerization flasks and were extracted with 200 mL THF for 2 weeks to remove the sol fraction. Next, the THF solution was recovered by filtration. The extraction procedure was repeated once more for 2 weeks, and the solvent from the combined extracts was evaporated using a rotary evaporator. The recovered polymer was further dried overnight in a vacuum oven at room temperature. The sol fraction was calculated as the ratio of the dried mass of the extracted polymer divided by the theoretical mass of the polymer in the conetwork. The latter was estimated from the polymerization stoichiometry as the sum of the masses of the monomers, the cross-linker, and the initiator. The dried extractables were subsequently characterized in terms of their MW and composition by GPC and ^{1}H NMR spectroscopy, respectively.

Hydrolysis of the THPMA Units in the Conetworks. After the extraction, a part of each conetwork was transferred to a 1 L glass jar, which contained 100 mL of THF plus 35 mL of an HCl (2 M) aqueous solution whose number of moles in HCl was more than twice the number of THPMA equivalents in the conetwork. The system was allowed to hydrolyze for 3 weeks, followed by washing with distilled water for another 2 weeks to remove THF, DHP, and excess HCl. The water was changed every day. A small sample from each conetwork was cut and dried under vacuum, and its FTIR spectrum was recorded.

Characterization of the Hydrolyzed Conetworks. *Fourier-Transform Infrared Spectroscopy.* The Fourier-transform infrared (FTIR) spectra of the conetworks were recorded using a Prestige-21 Shimadzu FTIR spectrometer equipped with an attenuated total reflectance (ATR) accessory.

Measurements of the Degree of Swelling (DS). The extracted and hydrolyzed conetworks swollen in water were cut into small pieces (1−2 cm^3) and dried under vacuum for 76 h. The mass of each dry conetwork sample was determined gravimetrically. Then the conetwork samples were transferred in THF or in water for DS measurements. One sample from each conetwork was swollen in THF, and 12 other samples were allowed to equilibrate in basic, neutral, and acidic Milli-Q (deionized) water for 2 weeks. In nine of the 12 samples, a precalculated volume of base (0.5 M NaOH standard solution) was added to obtain DIs between 15% and 100%. The calculation was based on the measured dry mass of each sample, from which the number of equivalents of MAA units was estimated (assuming that all MAA units were not ionized before the addition of NaOH). The pH of these nine samples covered the range between 8 and 12. One sample remained neutral (no acid or base was added) and had a pH around 5.5. Two samples were acidified by the addition of small volumes of a 0.5 M HCl standard solution. These samples were allowed to equilibrate for 3 weeks. The DSs were calculated as the ratio of the swollen conetwork mass divided by the dry conetwork mass. All DSs were determined five times, and the averages of the measurements are presented along with their 95% confidence intervals. After the DSs were determined in water as a function of pH, the water-swollen conetwork samples were dried in a vacuum oven at room temperature. The dried samples were transferred to THF and left to equilibrate for 3 weeks. The DSs of the THF-swollen conetworks were calculated from their gravimetrically determined masses.

Calculation of Degree of Ionization (DI) and the Effective pK. The DI of each sample was calculated as the number of NaOH equivalents added divided by the number of MAA unit equivalents present in the sample. The hydrogen ion titration curves were obtained by plotting the calculated DIs against the measured solution pH. The effective pK of the MAA units in each conetwork was estimated from the hydrogen ion titration curve as the pH (of the supernatant solution) at 50% ionization.

Small-Angle Neutron Scattering (SANS). All the (hydrolyzed) conetworks of this study were characterized using SANS in D_2O. The samples were in the uncharged state (pH $\sim$ 8). SANS measurements were performed on the 30 m NG7 instrument at the Center for Neutron Research of the National Institute of Standards and Technology (NIST). The incident wavelength was $\lambda = 6$ Å. Three sample-to-detector distances, 1.00, 4.00, and 15.30 m, were employed, covering a q range [$q = 4\pi/\lambda \sin(\theta/2)$] from 0.003 to 0.60 Å^{-1}. The samples were loaded in 1 mm gap thickness quartz cells. The scattering patterns were isotropic, and therefore, the measured counts were circularly averaged. The averaged data were corrected for empty cell and background. The distance between the scattering centers was estimated from the position of the intensity maximum, q_{max}, as $2\pi/q_{max}$.

Atomic Force Microscopy (AFM). The surfaces of the dried (hydrolyzed and uncharged) samples were microtomed at room temperature with a diamond knife from Diatome and a Microtom ULTRACUT UCT from Leica, removing serial sections of about 100 nm thickness from the surface, so that morphologies free of surface artifacts could be taken. AFM images of the microtomed samples were recorded with a Nanoscope III scanning probe microscope from Digital Instruments using Si cantilevers (tip radius about 5 nm) with a fundamental resonance frequency of ~200 kHz.

Results and Discussion

Polymerization Methodology. The synthesis of the model conetworks started with the preparation of block and statistical

Table 1. Molecular Weights and Compositions of the Linear Copolymer Precursors to the Conetworks

			GPC results		% mol THPMA	
conetwork no.	theoretical chemical structure[a]	theoretical MW	M_n	M_w/M_n	theoretical	^{1}H NMR
1	M_{32}	3400	5340	1.19		
	$T_{1.25}$-*b*-M_{32}-*b*-$T_{1.25}$	3825	5870	1.22	7	
2	M_{32}	3400	4340	1.20		
	$T_{2.5}$-*b*-M_{32}-*b*-$T_{2.5}$	4250	5130	1.22	14	
3	M_{32}	3400	4370	1.21		
	T_5-*b*-M_{32}-*b*-T_5	5100	5820	1.25	24	16
4	M_{32}	3400	5020	1.21		
	T_{10}-*b*-M_{32}-*b*-T_{10}	6800	8700	1.31	39	26
5	M_{32}	3400	4970	1.19		
	T_{15}-*b*-M_{32}-*b*-T_{15}	8500	9870	1.32	48	31
6	T_{20}	3594	4360	1.22		
	M_{16}-*b*-T_{20}-*b*-M_{16}	6800	9820	1.34	39	24
7	T_{20}-*co*-M_{32}	6800	9130	1.27	39	31
8	random−random	6800			39	
9	M_{20}	2197	2760	1.20		
	T_{10}-*b*-M_{20}-*b*-T_{10}	5599	5660	1.28	50	43
10	M_{10}	1195	1480	1.24		
	T_{10}-*b*-M_{10}-*b*-T_{10}	4598	5720	1.24	67	

[a] T and M are (further) abbreviations for THPMA (MAA) and MMA, respectively.

Table 2. Mass Percentage, Molecular Weights, and Compositions of the Sol Fractions Extracted from the Conetworks, as Measured by Gravimetry, GPC, and ^{1}H NMR

			GPC results		% mol THPMA		
					theoretical	by ^{1}H NMR	
conetwork no.	theoretical chemical structure[a]	extractables (w/w %)	M_n	M_w/M_n	of precursor	precursor	extractables
1	$T_{1.25}$-*b*-M_{32}-*b*-$T_{1.25}$	15	3600	1.33	7		0
2	$T_{2.5}$-*b*-M_{32}-*b*-$T_{2.5}$	19	3930	1.31	14		0
3	T_5-*b*-M_{32}-*b*-T_5	26	4610	1.27	24	16	0
4	T_{10}-*b*-M_{32}-*b*-T_{10}	38	6910	1.39	39	26	14
5	T_{15}-*b*-M_{32}-*b*-T_{15}	41	8590	1.32	48	31	24
6	M_{16}-*b*-T_{20}-*b*-M_{16}	24	11500	1.08	39	24	66
7	T_{20}-*co*-M_{32}	30	6700	1.38	39	31	25
8	random−random	4.4	8000	1.21	39		0
9	T_{10}-*b*-M_{20}-*b*-T_{10}	24	5300	1.30	50	43	25
10	T_{10}-*b*-M_{10}-*b*-T_{10}	19	5200	1.31	67		49

[a] T and M are (further) abbreviations for THPMA (MAA) and MMA, respectively.

copolymers with well-defined length, i.e., with narrow MWD and exact bifunctionality. Thus, these polymers should possess the capability of further growth at both ends. This was achieved by applying a bifunctional initiator, MTSCH (see Figure 1), for the GTP of the selected monomers with a predetermined addition sequence (Figure 2) and relative amounts. The synthetic routes for the peparation of structurally different conetworks are outlined in Figure 3. As shown in this figure, model conetworks were prepared from ABA and BAB triblock copolymers and an A−B statistical copolymer, where A and B are THPMA and MMA, respectively. After copolymerization, the EGDMA bifunctional monomer was added, which led to cross-linked polymers by multifunctional core formation. For comparison, a randomly cross-linked statistical copolymer conetwork was also prepared by the simultaneous copolymerization of MMA, THPMA, and the EGDMA cross-linker.

The composition of the conetworks was varied from 7 to 70 mol % of MAA units. The linear precursors to the conetworks are illustrated schematically in Figure 4. The MMA and the MAA units are colored in black and white, respectively, while the EGDMA units are indicated by a gray circle.

Molecular Weights and Composition. Table 1 shows the MWs and compositions of the linear precursors to the conetworks as measured by GPC and ^{1}H NMR, respectively. The number-average molecular weights, M_ns, were slightly higher than the theoretically calculated MWs probably due to partial deactivation of the initiator. The MWDs were found to be narrow, with polydispersity indices (M_w/M_n) lower than 1.35. It is noteworthy that the M_ns of the copolymer precursors were always higher than those of the corresponding homopolymer precursors to the conetworks, indicating block copolymer formation. Also, the MWDs of the linear copolymer precursors were monodisperse, without any traces of the corresponding homopolymer precursors. The compositions of the copolymer precursors were determined from the ^{1}H NMR spectra (not shown), by the integral ratio of the signals from the three methoxy protons of MMA (3.6 ppm) to the one ester acetal proton of THPMA (5.9 ppm). The THPMA compositions were found to be lower than the compositions expected on the basis of comonomer feed ratio. This was most likely due to spontaneous partial deprotection of the THPMA units during the 3 day vacuum-drying of the linear copolymer precursors before the NMR measurement. The alternate explanation of incomplete THPMA polymerization is totally excluded, as GPC analyses indicated complete monomer conversion in all cases.

Percentage, MW, and Composition of the Sol Fraction of the Conetworks. Table 2 shows the mass percentage, M_ns, M_w/M_ns, and composition of the extractables from each conetwork as measured by gravimetry, GPC, and ^{1}H NMR. With the exceptions of conetwork 4 and conetwork 5, the sol fractions of the conetworks were lower than 30% w/w. It seems that the highest percentages of extractables were obtained from the conetworks with the highest degree of polymerization (DP) and where the THPMA monomer was added right before cross-linking. The latter might be due to the better cross-reactivity of the MMA−EGDMA pair compared to that of the THPMA−

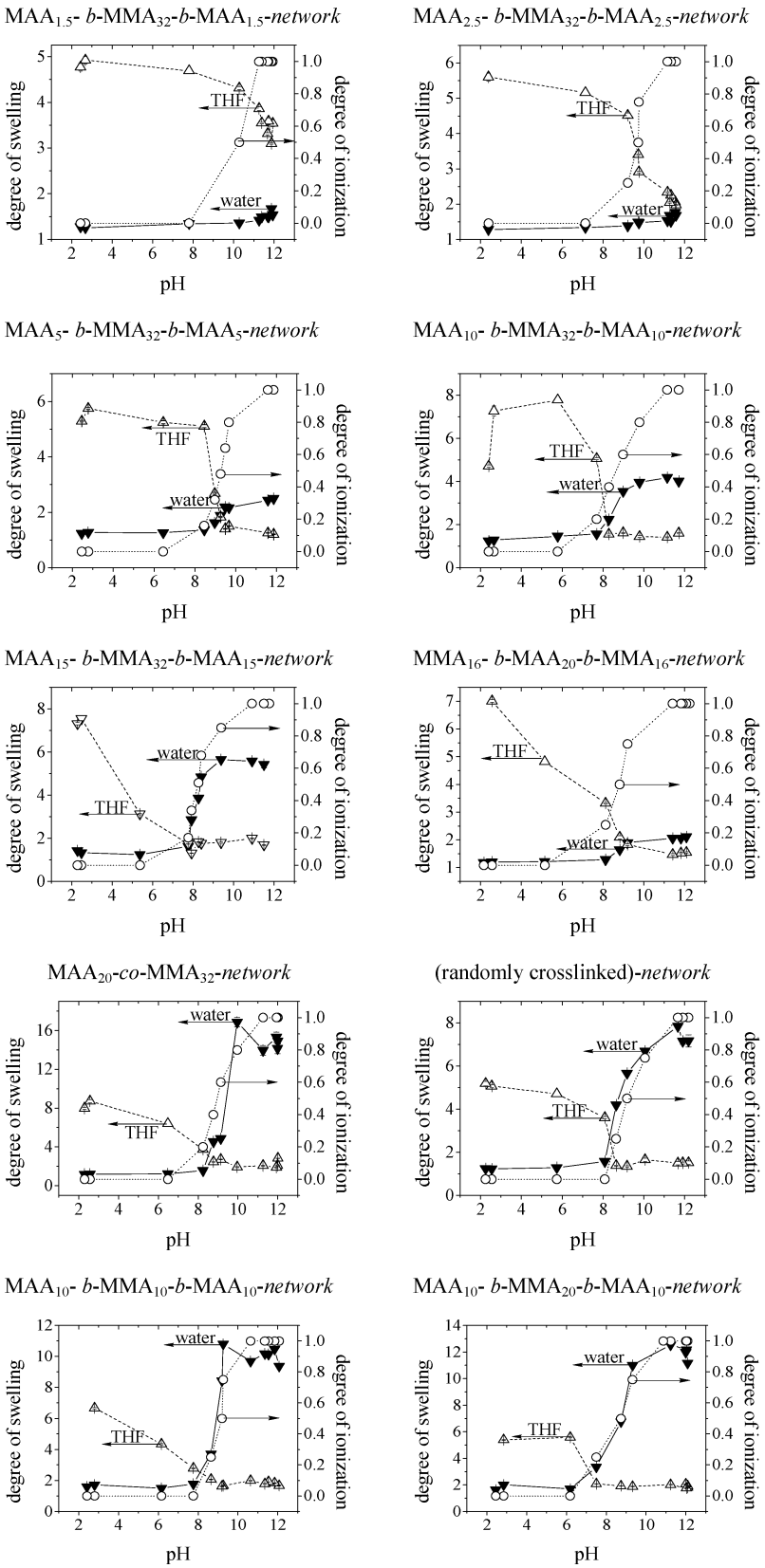

Figure 5. Degrees of swelling and degrees of ionization of all the conetworks in this study as a function of pH.

EGDMA pair. From the M_ns and the composition of the extractables, the step where the highest deactivation occurred during synthesis could be inferred. For all the conetworks, this was the first, homopolymerization, step because the extractables had a lower M_n and were also richer in the monomer polymerized first, as compared to the linear triblock precursors.

Yields of Cross-Linker Polymerization and THPMA Hydrolysis. To convert the THPMA units to MAA units, acid hydrolysis, rather than thermolysis, was used.[26,36] Acid hydrolysis provides a cleaner route to deprotection than thermolysis[36,37] due to the tendency of the latter to lead to partial anhydride formation.[39,40] The conversion to MAA units was confirmed

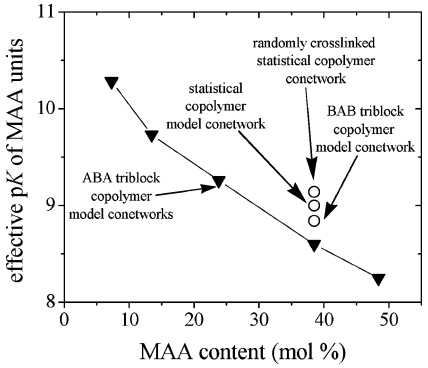

Figure 6. Dependence of the effective p*K*s of the MAA units in the conetworks on the MAA content.

qualitatively by FTIR from the appearance of a double peak at 2940−2860 cm^{-1} due to the stretching vibration of the OH group of MAA. The ATR-FTIR spectra also indicated full conversion of the vinyl groups of the cross-linker due to the absence of the signal at 1637 cm^{-1}. It seems, therefore, that the GTP enolate anion is reactive enough to both vinyl groups of EGDMA. This must be contrasted to the radical polymerization of EGDMA, in which double-bond conversion is delayed because the polymerization reactivity of the second vinyl group is very much reduced once the first vinyl group has polymerized.

Degrees of Swelling and Ionization. The experimentally measured DSs in water and in THF and the DIs of all the conetworks are plotted against pH in Figure 5. The DSs in the two solvents followed opposite pH dependencies. In water, the conetworks started to swell above pH 7.5 due to the ionization of the MAA units and the compatibility of the resulting sodium methacrylate (Na^+MA^-) units with water. Under these conditions, the electrostatic repulsive forces between the backbones due to the negative charge on the MA^- units, and the presence of the Na^+ counterions to the carboxylate groups, both drive conetwork swelling.[20,41,42] The aqueous DSs presented a maximum at pH 9−11, followed by a plateau, or even a small decrease, at higher pH values, which was probably due to the increase in the ionic strength effected by the relatively high concentration of NaOH under these conditions.[42] The hydrogen ion titration curves are also shown in the same graphs. These curves followed the corresponding aqueous DS vs pH curves, confirming the electrostatic origin of swelling.

In THF, the conetworks showed exactly the opposite tendencies. In this solvent, the DSs decreased as the pH and the DIs increased. This was due to the incompatibility of THF with the Na^+MA^- units. The incompatibility of charged units with organic solvents of low dielectric constant, such as THF, is referred to as the "ionomer effect", which has already been reported for networks with ionized carboxylic acid units equilibrated in various organic solvents and solvent mixtures.[43−47]

The plots in Figure 5 were used to extract the DSs in water and in THF both in the uncharged and in the fully ionized states as well as the effective p*K*s of the MAA units in the conetworks, which are presented and discussed in the following sections.

Effective pKs of the MAA Units. The dependence of the effective p*K*s of the MAA units in the conetworks on the MAA content is shown in Figure 6. The effective p*K* values decreased as the MAA content of the conetworks increased or, equivalently, as the MMA content decreased. In other words, MAA became a stronger acid as the conetworks became less hydrophobic. A decrease in the MMA content caused an increase in the hydrophilicity and in the dielectric constant of the conetworks, rendering ionization easier, which resulted in the lowering of the effective p*K*.[42] This has also been observed before for other amphiphilic conetworks based on the hydrophobic MMA and the positively ionizable DMAEMA.[25] However, since DMAEMA is a weak base rather than a weak acid, the effective p*K* values of the DMAEMA units in those conetworks were raised (became a stronger base) as the hydrophobicity was lowered. It is noteworthy that no clear architecture dependence of the p*K* was observed, since the four equimolar conetworks with different architectures presented similar p*K* values. The effective p*K* values of these conetworks are higher than those reported in the literature for MAA homopolymer networks of p$K = 6.8$, as expected.[48]

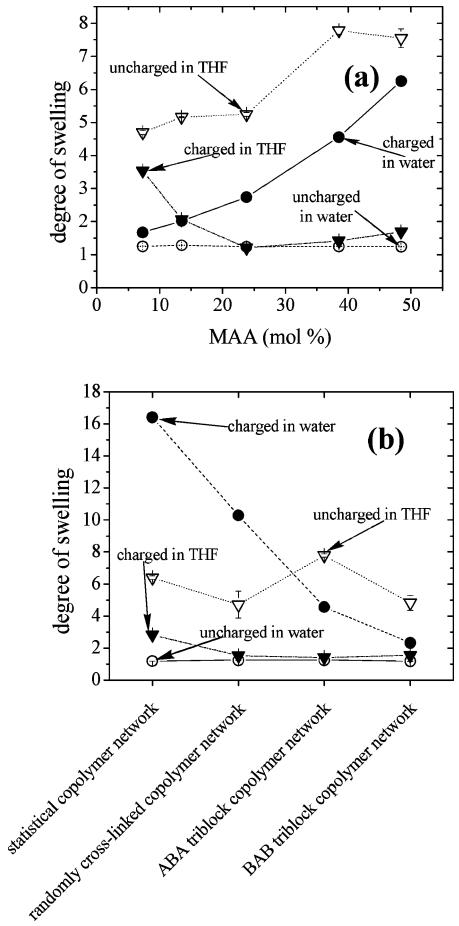

Figure 7. Degrees of swelling of the conetworks in water and in THF for uncharged and fully charged MAA units. Effects of (a) conetwork composition and (b) conetwork architecture.

Table 3. Monomer Unit Compatibility with the Two Solvents[a]

	solvent	water	THF
monomer unit	MMA	×	√
	uncharged MAA	∼×	√
	charged MAA	√	×

[a] Key: √ = compatible; × = incompatible; ∼× = marginally compatible.

DSs in Water and in THF in the Uncharged and the Fully Ionized States. The DSs of the conetworks in water and in THF in the nonionized (pH around 2) and the fully ionized (pH around 11) states are summarized in Figure 7. Figure 7a shows the effect of conetwork composition while Figure 7b presents the effect of conetwork architecture. The composition dependence of the DSs in Figure 7a can be interpreted according to Tables 3 and 4, which list the compatibility of the conetwork units, MAA (both charged and uncharged states) and MMA, with the two solvents, water and THF, and the number of

Table 4. Number of Compatible Conetwork Components in the Two Solvents

	water	THF
MMA−uncharged MAA	~0	2
MMA−charged MAA	1	1

compatible (swelling) components in each solvent. The highest DSs were observed in THF for uncharged MAA units where both types of units, MMA and uncharged MAA, were solvent-compatible. The lowest DSs were measured also for uncharged MAA units but in water, with which MMA is incompatible and MAA is marginally compatible. Intermediate DSs were found for charged MAA units in either solvent where one component was solvent-compatible. The detailed swelling trends and their interpretation are as follows:

(i) DSs in water at low pH (uncharged MAA): No dependence of the DS on composition was observed because the conetworks were totally collapsed, with both components dehydrated and practically no swelling.

(ii) DSs in water at high pH (fully charged MAA): A large increase of the DS with the MAA content was observed due to the great compatibility of water with charged MAA (Na^+MA^-). A reason for extra swelling was the increase in the (average) MW between the cross-links, M_c, accompanying the increase in the MAA/Na^+MA^- content.

(iii) DSs in THF with fully charged MAA (Na^+MA^-): A large decrease followed by a slight increase of the swelling as the MAA content went up was observed, forming a shallow minimum at a 24 mol % MAA content. The initial decrease in the DS can be attributed to the increase in the content of the solvent-incompatible MAA (Na^+MA^-) units. The final increase was due to the increase in M_c accompanying the increase in the MAA content. Note the crossing of the DS curves of fully charged conetworks in THF and water at 15% MAA content, effected by the opposite effects of the MAA content on the swelling in the two solvents.

(iv) DS in THF with uncharged MAA: High DSs were observed because both types of units were compatible with the solvent. A gradual increase in the DSs in THF with the MAA content occurred because of the increase in M_c accompanying the increase in the MAA content.

Figure 7b focuses on the effect of the conetwork architecture on the DSs. For uncharged MAA units in water, all the conetworks were collapsed, exhibiting minimal DSs, and therefore, no conetwork architecture effect on swelling could be detected. However, for fully charged MAA units in water, the architecture had a strong influence on the DSs. In particular, the statistical copolymer model conetwork swelled 4−8 times more than the triblock copolymer model conetworks and almost twice as high as the randomly cross-linked conetwork. This architecture dependence of the DSs can be attributed to the different phase behavior of the two triblock copolymer-based model conetworks compared to the other two statistical copolymer-based conetworks. In the triblock copolymer-based model conetworks, there is phase separation, resulting in the shrinkage of one type of blocks (hydrophobic MMA in water or Na^+MA^- salt in THF) and to lower DSs. In contrast, in the statistical copolymer conetworks, the random distribution of the two comonomers in the copolymer chains precludes segregation and the DSs remain relatively high. It is visualized that, in this type of conetwork, the solvated units drag along the nonsolvated units, forcing them to also contribute to swelling. The two equimolar triblock copolymer model conetworks in this work presented different aqueous DSs in the charged state. In particular, the conetwork based on the PMMA−PMAA−PMMA triblock copolymer presented a lower DS at high pH than the conetwork with the reverse architecture, indicating that when the hydrophobic MMA blocks are adjacent to the hydrophobic cross-links, a greater reduction in the effective chain length is accomplished. Comparing the two less-ordered conetwork architectures, the randomly cross-linked statistical copolymer conetwork swelled less than the statistical copolymer model conetwork. This can be attributed to the lower M_c in this conetwork, resulting from the random distribution of the cross-linker. In contrast, in the statistical conetwork, the cross-linkers were concentrated at the chain ends (four cross-linker residues per chain end), leading to higher M_cs.

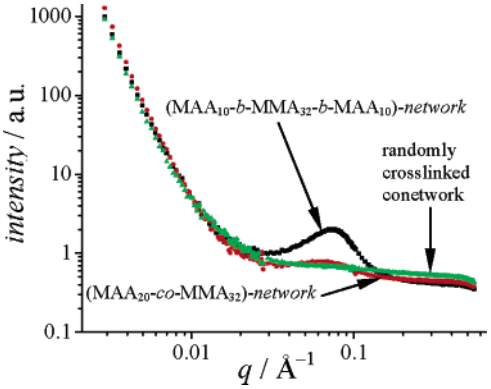

Figure 8. SANS profiles of the three isomeric conetworks in D_2O in the uncharged state.

The DSs in THF of the isomeric conetworks in the uncharged state did not show a significant dependence on conetwork architecture, since THF is a nonselective solvent. In the case of fully ionized MAA units in THF, the conetworks were in a collapsed state for all the architectures.

Nanophase Behavior. In the following, we provide the results of a preliminary investigation on the phase behavior of the conetworks, using both SANS and AFM. To the best of our knowledge, this is the first time that these techniques are combined in a single investigation for the elucidation of the structure of covalent APCNs, although there are two reports from Ryan's group where small-angle X-ray scattering (SAXS) and AFM were used to characterize noncovalent networks.[49,50] SAXS and AFM investigations were also carried out on poly(2-hydroxyethyl methacrylate)-*l*-polyisobutylene covalent conetworks.[4] A SANS study on poly(ethyl acrylate)-*l*-polyisobutylene[21a] and an AFM study on several conetworks have also been reported recently.[4,21d,e,22]

SANS. Figure 8 shows the SANS profiles of three isomeric conetworks in the uncharged state in D_2O: the model conetwork based on the triblock copolymer MAA_{10}-*b*-MMA_{32}-*b*-MAA_{10}, the model conetwork based on the statistical copolymer MAA_{20}-*co*-MMA_{32}, and the randomly cross-linked conetwork MAA_{20}-*co*-MMA_{32}-*co*-$EGDMA_8$. The SANS profiles of the three conetworks differed only in the intermediate q range, from 0.02 to 0.20 $Å^{-1}$. In particular, the model conetwork based on the triblock copolymer presented an intense peak, indicating phase separation. The absence of higher harmonics can be attributed to the polydispersity of the scattering centers or/and to their short-range liquidlike order.[50] The distance between the scattering domains (assuming spherical geometry) for this triblock copolymer-based conetwork was calculated to be 8.7 nm. The absence of scattering peaks in the two statistical conetworks (the model and the randomly cross-linked) can be attributed to the random distribution of the hydrophobic units in the chains of these conetworks, which precludes phase

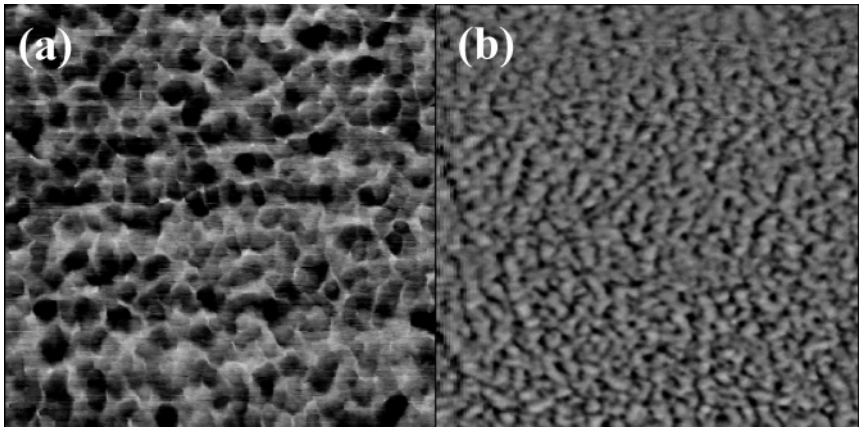

Figure 9. AFM phase mode images for **(**a**)** the triblock and **(**b**)** the statistical copolymer-based model conetworks. Image size of both 500×500 nm^2.

separation. The shallow shoulder in the profile of the statistical copolymer-based model conetwork is probably due to the presence of relatively large EGDMA cores (in the model conetworks all cross-linker was polymerized last), while the complete absence of shoulder in the randomly cross-linked conetwork is due to the absence of EGDMA cores, since EGDMA is randomly distributed within this conetwork.

AFM. Figure 9 displays AFM images for the triblock and statistical copolymer-based model conetworks in the uncharged state in the bulk. The images were measured in phase mode, which distinguishes between hard (bright) and soft (dark) phases. The model conetwork based on the triblock copolymer MAA_{10}-*b*-MMA_{32}-*b*-MAA_{10} displays large spherical domains of a size of ~40 nm, whereas the model conetwork based on the statistical copolymer MAA_{20}-*co*-MMA_{32} exhibits smaller and elongated domains of a broadly distributed size in a range of 4−20 nm with the average of some 10 nm. The domain size of 40 nm in the former conetwork is larger than the characteristic size of 9 nm determined by SANS. This indicates that the contrast difference between the phases is not high enough to see distinguishable morphologies in the higher resolution. Note that both polymer phases are below their glass transition temperatures (T_g). It is possible that the large domains seen in Figure 9a are phase separated as well. Thus, the SANS measurements can give complementary information to AFM. The domain size of 10 nm in the statistical copolymer model conetwork corresponds to the EGDMA cores and is in perfect agreement with the SANS measurements. The wide distribution of the irregular morphology explains the weak and broad neutron scattering signal seen in Figure 8.

Conclusions

A series of model amphiphilic polymer conetworks were successfully synthesized using the controlled technique group transfer polymerization. The prepared conetwork series covered a wide range of compositions and architectures. The degrees of swelling (DS) were determined in water and in THF, and the effect of methacrylic acid (MAA) ionization and conetwork composition and architecture were investigated. The DSs in water were found to increase with the pH and with the MAA content, as expected. In THF, an opposite dependence was determined, and the DSs decreased with increasing the degree of ionization of the MAA units. Architecture was also found to have an important effect on the DSs in water. In particular, the statistical copolymer model conetwork, which was unable to nanophase separate, swelled more than the triblock copolymer-based model conetworks. The DSs in THF were only affected by the degree of polymerization of the elastic chains between the cross-links and not by the conetwork architecture. Small-angle neutron scattering and atomic force microscopy indicated nanophase separation within conetworks based on triblock copolymers and lack of structure within conetworks based on the statistical copolymers.

Acknowledgment. The European Commission is gratefully acknowledged for providing a Marie Curie grant (HPMT-CT-2001-00421) that enabled the stay of G.K. at the University of Cyprus. The A. G. Leventis Foundation is thanked for a generous donation that enabled the purchase of the NMR spectrometer of the University of Cyprus. We also thank our colleagues Dr. P. A. Koutentis and Ms. I. Christoforou for providing access and analyzing for us conetwork samples on their ATR-FTIR spectrometer. The Hungarian Scientific Research Fund (OTKA T46759 and IN64295) is also acknowledged. Finally, we acknowledge the support of the National Institute of Standards and Technology (NIST), U.S. Department of Commerce, in providing the neutron research facilities used in this work. The mention of commercial equipment or materials does not imply endorsement by NIST.

References and Notes

(1) Patrickios, C. S.; Georgiou, T. K. *Curr. Opin. Colloid Interface Sci.* **2003**, *8*, 76−85.
(2) Erdödi, G.; Kennedy, J. P. *Prog. Polym. Sci.* **2006**, *31*, 1−18.
(3) Bruns, N.; Tiller, J. C. *Nano Lett.* **2005**, *5*, 45−48.
(4) Scherble, J.; Thomann, R.; Iván, B.; Mülhaupt, R. *J. Polym. Sci., Part B: Polym. Phys.* **2001**, *39*, 1429−1436.
(5) Iván, B.; Kennedy, J. P.; Mackey, P. W. In *Polymeric Drugs and Drug Delivery Systems*; Dunn, R. L., Ottenbrite, R. M., Eds.; ACS Symposium Series 469; American Chemical Society: Washington, DC, 1991; pp 194−202.
(6) Iván, B.; Kennedy, J. P.; Mackey, P. W. In *Polymeric Drugs and Drug Delivery Systems*; Dunn, R. L.; Ottenbrite, R. M., Eds.; ACS Symposium Series 469. American Chemical Society: Washington, DC, 1991; pp 203−212.
(7) Barakat, I.; Dubois, Ph.; Grandfils, Ch.; Jérôme, R. *J. Polym. Sci., Part. A: Polym. Chem.* **1999**, *37*, 2401−2411.
(8) Zhu, C.; Hard, C.; Lin, C. P.; Gitsov, I. *J. Polym. Sci., Part A: Polym. Chem.* **2005**, *43*, 4017−4029.
(9) Behravesh, E.; Jo, S.; Zygourakis, K.; Mikos, A. G. *Biomacromolecules* **2002**, *3*, 374−381.
(10) Haigh, R.; Fullwood, N.; Rimmer, S. *Biomaterials* **2002**, *23*, 3509−3516.
(11) Rimmer, S.; German, M. J.; Maughan, J.; Sun, Y.; Fullwood, N.; Ebdon, J.; MacNeil, S. *Biomaterials* **2005**, *26*, 2219−2230.
(12) Alexandre, E.; Schmitt, B.; Boudjema, K.; Merrill, E. W.; Lutz, P. J. *Macromol. Biosci.* **2004**, *4*, 639−648.
(13) Nicolson, P. C.; Vogt, J. *Biomaterials* **2001**, *22*, 3273−3283.
(14) (a) Erdödi, G.; Kennedy, J. P. *J. Polym. Sci., Part A: Polym. Chem.* **2005**, *43*, 4965−4971. (b) Erdödi, G.; Kennedy, J. P. *J. Polym. Sci.,*

Part A: Polym. Chem. **2005**, *43*, 3491−3501. (c) He, C. J.; Erdödi, G.; Kennedy, J. P. *J. Polym. Sci., Part B: Polym. Phys.* **2006**, *44*, 1474−1481. (d) Erdödi, G.; Kennedy, J. P. *J. Polym. Sci., Part A: Polym. Chem.* **2005**, *43*, 4953−4964. (e) Nugay, N.; Erdödi, G.; Kennedy, J. P. *J. Polym. Sci., Part A: Polym. Chem.* **2005**, *43*, 630−637. (f) Erdödi, G.; Iván, B. *Chem. Mater.* **2004**, *16*, 959−962.

(15) (a) Guan, Y.; Jiang, W. W.; Zhang, W. C.; Wan, G. X.; Peng, Y. X. *J. Polym. Sci., Part A: Polym. Chem.* **2001**, *39*, 1784−1790. (b) Guan, Y.; Jiang, W. W.; Zhang, W. C.; Wan, G. X.; Peng, Y. X. *J. Appl. Polym. Sci.* **2002**, *85*, 351−357. (c) Tiller, J. C.; Sprich, C.; Hartmann, L. *J. Controlled Release* **2005**, *103*, 355−367. (d) Tiller, J. C.; Hartmann, L.; Scherble, J. *Surf. Coat. Int.: Part B: Coatings Trans.* **2005**, *88*, 49−53. (e) Haraszti, M.; Tóth, E.; Iván, B. *Chem. Mater.* **2006**, *18*, 4952−4958.

(16) Gudipati, C. S.; Finlay, J. A.; Callow, J. A.; Callow, M. E.; Wooley, K. L. *Langmuir* **2005**, *21*, 3044−3053.

(17) Brown, G. O.; Bergquist, C.; Ferm, P.; Wooley, K. L. *J. Am. Chem. Soc.* **2005**, *127*, 11238−11239.

(18) Du Prez, F. E.; Goethals, E. J.; Schué, R.; Qariouh, H.; Schué, F. *Polym. Int.* **1998**, *46*, 117−125.

(19) Carrot, G.; Schmitt, B.; Lutz, P. *Polym. Bull. (Berlin)* **1998**, *40*, 181−188.

(20) Vamvakaki, M.; Patrickios, C. S. *J. Phys. Chem. B* **2001**, *105*, 4979−4986.

(21) (a) Iván, B.; Almdal, K.; Mortensen, K.; Johannsen, I.; Kops, J. *Macromolecules* **2001**, *34*, 1579−1585. (b) Domján, A.; Erdödi, G.; Wilhelm, M.; Neidhöfer, M.; Iván, B.; Spiess, H. W. *Macromolecules* **2003**, *36*, 9107−9114. (c) Lequieu, W.; Van De Velde, P.; Du, Prez, F. E.; Adriaensens, P.; Storme, L.; Gelan, J. *Polymer* **2004**, *45*, 7943−7951. (d) Bruns, N.; Scherble, J.; Hartmann, L.; Thomann, R.; Iván, B.; Mülhaupt, R.; Tiller, J. C. *Macromolecules* **2005**, *38*, 2431−2438. (e) Iván, B.; Haraszti, M.; Erdödi, G.; Scherble, J.; Thomann, R.; Mülhaupt, R. *Macromol. Symp.* **2005**, *227*, 265−273.

(22) Bruns, N.; Tiller, J. C. *Macromolecules* **2006**, *39*, 4386−4394.

(23) Triftaridou, A. I.; Kafouris, D.; Vamvakaki, M.; Georgiou, T. K.; Krasia, T. C.; Themistou, E.; Hadjiantoniou, N.; Patrickios, C. S. *Polym. Bull. (Berlin)* **2007**, *58*, 185−190.

(24) Simmons, M. R.; Yamasaki, E. N.; Patrickios, C. S. *Macromolecules* **2000**, *33*, 3176−3179.

(25) Triftaridou, A. I.; Hadjiyannakou, S. C.; Vamvakaki, M.; Patrickios, C. S. *Macromolecules* **2002**, *35*, 2506−2513.

(26) Demosthenous, E.; Hadjiyannakou, S. C.; Vamvakaki, M.; Patrickios, C. S. *Macromolecules* **2002**, *35*, 2252−2260.

(27) Loizou, E.; Triftaridou, A. I.; Georgiou, T. K.; Vamvakaki, M.; Patrickios, C. S. *Biomacromolecules* **2003**, *4*, 1150−1160.

(28) Vamvakaki, M.; Patrickios, C. S. *Chem. Mater.* **2002**, *14*, 1630−1638.

(29) Hild, G. *Prog. Polym. Sci.* **1998**, *23*, 1019−1149.

(30) Webster, O. W. *Science* **1991**, *251*, 887−893.

(31) Webster, O. W.; Hertler, W. R.; Sogah, D. Y.; Farnham, W. B.; RajanBabu, T. V. *J. Am. Chem. Soc.* **1983**, *105*, 5706−5708.

(32) Sogah, D. Y.; Hertler, W. R.; Webster, O. W.; Cohen, G. M. *Macromolecules* **1987**, *20*, 1473−1488.

(33) Dicker, I. B.; Cohen, G. M.; Farnham, W. B.; Hertler, W. R.; Laganis, E. D.; Sogah, D. Y. *Macromolecules* **1990**, *23*, 4034−4041.

(34) Webster, O. W. *J. Polym. Sci., Part A: Polym. Chem.* **2000**, *38*, 2855−2860.

(35) Webster, O. W. *Adv. Polym. Sci.* **2004**, *167*, 1−34.

(36) Kearns, J. E.; McLean, C. D.; Solomon, D. H. *J. Macromol. Sci., Chem.* **1974**, *A8*, 673−685.

(37) Hertler, W. R. U.S. Patent 5,072,029, 1991.

(38) Steinbrecht, K.; Bandermann, F. *Makromol. Chem.* **1989**, *190*, 2183−2191.

(39) Lowe, A. B.; Billingham, N. C.; Armes, S. P. *Chem. Commun.* **1997**, 1035−1036.

(40) Lowe, A. B.; Billingham, N. C.; Armes, S. P. *Macromolecules* **1998**, *31*, 5991−5998.

(41) Georgiou, T. K.; Vamvakaki, M.; Patrickios, C. S. *Polymer* **2004**, *45*, 7341−7355.

(42) Philippova, O. E.; Hourdet, D.; Audebert, R.; Khokhlov, A. R. *Macromolecules* **1997**, *30*, 8278−8285.

(43) Tanaka, T. *Sci. Am.* **1981**, *244* (1), 124−138.

(44) Ilavsky, M. *Macromolecules* **1982**, *15*, 782−788.

(45) Nicoli, D.; Young, C.; Tanaka, T.; Pollak, A.; Whitesides, G. *Macromolecules* **1983**, *16*, 887−890.

(46) Philippova, O. E.; Sitnikova, N. L.; Demidovich, G. B.; Khokhlov, A. R. *Macromolecules* **1996**, *29*, 4642−4645.

(47) Kawaguchi, D.; Satoh, M. *Macromolecules* **1999**, *32*, 7828−7835.

(48) Georgiades, S. N.; Vamvakaki, M.; Patrickios, C. S. *Macromolecules* **2002**, *35*, 4903−4911.

(49) Howse, J. R.; Topham, P.; Crook, C. J.; Gleeson, A. J.; Bras, W.; Jones, R. A. L.; Ryan, A. J. *Nano Lett.* **2006**, *6*, 73−77.

(50) Topham, P. D.; Howse, J. R.; Mykhaylyk, O. O.; Armes, S. P.; Jones, R. A. L.; Ryan, A. J. *Macromolecules* **2006**, *39*, 5573−5576.

MA062400Y